1971SoPh...18..258P

GAS-MAGNETIC FIELD INTERACTIONS IN THE SOLAR CORONA

G. W. PNEUMAN and ROGER A. KOPP

High Altitude Observatory, National Center for Atmospheric Research, Boulder, Colo., U.S.A.*

(Received 26 November, 1970)

Abstract. It is evident from eclipse photographs that gas-magnetic field interactions are important in determining the structure and dynamical properties of the solar corona and interplanetary medium. Close to the Sun in regions of strong field, the coronal gas can be contained within closed loop structures. However, since the field in these regions decreases outward rapidly, the pressure and inertial forces of the solar wind eventually dominate and distend the field outward into interplanetary space. The complete geometrical and dynamical state is determined by a complex interplay of inertial, pressure, gravitational, and magnetic forces. The present paper is oriented toward the understanding of this interaction. The 'helmet' streamer type configuration with its associated neutral point and sheet currents is of central importance in this problem and is, therefore, considered in some detail.

Integration of the relevant partial differential equations is made tractable by an iterative technique consisting of three basic stages, which are described at length. A sample solution obtained by this method is presented and its physical properties discussed.

1. Introduction

In order to describe realistically the behavior of the coronal plasma as it expands out into interplanetary space, it is necessary to account for the interaction of this material with magnetic fields. That this is so is convincingly demonstrated in many eclipse photographs which show large regions of the inner corona dominated by magnetic fields. Within 2 $R_\odot$, large closed loop structures are visible which presumably prohibit local expansion. Even in regions of open magnetic field lines, the expansion is highly nonradial due to the influence of magnetic forces. Beyond about 2 $R_\odot$, the solar wind begins to dominate, distending the field more or less radially outward.

The overall structure of the solar corona and interplanetary medium is determined by the coronal heating mechanism and by a complex balance of pressure, gravitational, inertial, and magnetic forces. Evidently the magnetic forces dominate in the inner corona whereas the inertia of the solar wind determines the streamline configuration at large distances. In this study, we investigate this gas-magnetic field interaction in some detail within the framework of a theoretical model. Admittedly, the field configurations considered here are simple. Nevertheless, the relevant physics can be understood within the context of these simple geometries. Moreover, the method of solution described here can be directly extended to treat more realistic solar conditions.

2. Physical Considerations

In the absence of a magnetic field, the properties of the solar wind (subject to a specified heating model) are uniquely determined by the density and temperature at the

* The National Center for Atmospheric Research is sponsored by the National Science Foundation.

Solar Physics **18** (1971) 258–270. *All Rights Reserved*
Copyright © 1971 by D. Reidel Publishing Company, Dordrecht-Holland

© Kluwer Academic Publishers • Provided by the NASA Astrophysics Data System

1971SoPh...18..258P

coronal base in addition to the requirement that these quantities vanish at large distances. When a field is included, the normal component of that field must also be specified as a base condition. This, of course, introduces a latitude and longitude dependence of the solution as well as a high degree of nonradialness. Also, due to the influence of the magnetic field, the base density and temperature will not, in general, be uniform over the solar surface but will be influenced to some extent by the magnetic field distribution. Recent comparisons of the observed density structure in the lower corona with computed potential magnetic fields (Newkirk and Altschuler, 1970) suggest that this may be possibly due to the influence of the field on coronal heating (Osterbrock, 1961; Kuperus, 1965).

One type of configuration should be discussed in some detail before going on to the general solution of the problem stated above. This configuration is the so-called 'helmet' streamer which overlies large diffuse bipolar magnetic regions on the Sun. The helmet streamer consists of a region of closed magnetic loops with open field lines adjacent to and above the loops. It is commonly observed during solar eclipses and is schematically sketched in Figure 1. The chief theoretical interest in this structure lies in the neutral point occurring at the top of the closed loops and in the sheet currents both above and below the neutral point. In discussing these aspects, let us first compare the gross properties of the open and closed regions.

Under coronal conditions, the magnetic field is effectively frozen into the material. We surmise that, in the region of closed field lines, coronal expansion is not taking place. Hence, the gas is in magnetostatic equilibrium with the gas pressure being given by the equation of hydrostatic equilibrium applied *along* the field lines.* We neglect radiative losses and, since the thermal conductivity in a direction perpendicular to the field is extremely small, conductive losses are also precluded. As a result, we expect the temperature along closed field lines to be approximately constant.

In the open field line region, both expansion and outward heat conduction are taking place. These energy losses cause the temperature to decline outward there, and the scale height correspondingly falls relative to that in the adjacent closed region.

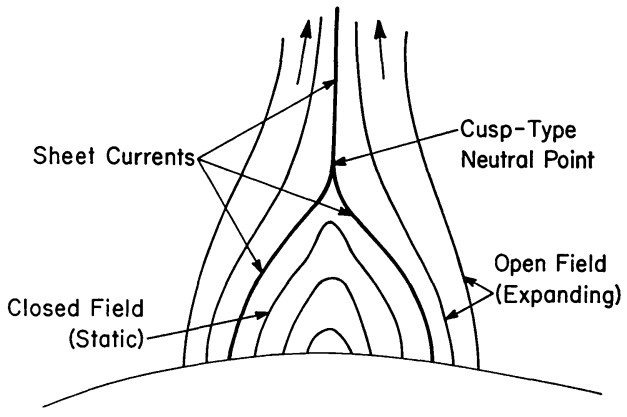


Fig. 1. Schematic diagram of a typical helmet streamer configuration.

* We do not consider here the distinct possibility of flow occurring along a closed loop because of pressure and temperature inequalities at the two foot points (Meyer and Schmidt, 1968).

© Kluwer Academic Publishers • Provided by the NASA Astrophysics Data System

1971SoPh...18..258P

This is directly responsible for the large observed outward increase in density enhancement in coronal streamers (Pneuman and Kopp, 1970).

A sheet current exists between the regions of opposite magnetic polarity above the neutral point. Similar surface currents are also necessary between the open and closed regions below the neutral point. The necessity for the existence of these lower sheet currents arises from the pressure discontinuity across the interface between these regions. The pressure jump exists because the expansion pulls down the pressure on the open field lines relative to that on the immediately adjacent closed field lines. Now, $p+B^2/8\pi$ must be continuous across the interface. Hence, a jump in the magnetic field strength is required to balance this pressure discontinuity. This jump in field strength must be associated (in the limit of infinite electrical conductivity) with a sheet current. Interestingly, the actual thickness of this sheet may depend not only upon the electrical conductivity (due to the discontinuity in magnetic field strength), but also upon the viscosity since the velocity is discontinuous.

The field configuration in the vicinity of the neutral point can theoretically be of three types – 'y', 'inverted T', and 'cusp' (Sturrock and Smith, 1968). However, two of these can be ruled out by physical considerations. The 'y-type' neutral point cannot occur since, for this case, the field vanishes when approaching the neutral point from all directions and there is consequently no way to balance the pressure jump between the open and closed regions. In the 'inverted T-type' neutral point, the field vanishes in the open region but not in the closed region and the jump in B is of the wrong sign. The only type of neutral point consistent with the mechanical forces is the 'cusp-type', in which the field goes to zero approaching the neutral point from the inside, but does not vanish on open field lines. The condition to be met there can, therefore, be mathematically stated as

$$p_c = p_s + B_s^2/8\pi\,, \tag{1}$$

where the subscript c refers to the closed region and the subscript s to the streaming region.

Finally, we derive another interesting property of the neutral point. Let us write the expressions for the conservation of mass and momentum along the field in the form

$$\frac{\partial}{\partial s}(NVS) = 0 \tag{2}$$

$$mNV\frac{\partial V}{\partial s} = -\frac{\partial p}{\partial s} - \frac{GM_\odot m}{r^2} N\cos\alpha \tag{3}$$

where S is the flux tube cross-section, s the arc length along the field, N the total particle density, V the expansion velocity, p the pressure, G the gravitation constant, $M_\odot$ the solar mass, m the mean particle mass, r the radial distance from the solar center, and α the angle between the streamline and the radius vector. Note that, since $\mathbf{J}\times\mathbf{B}$ is perpendicular to $\mathbf{B}$, the magnetic field does not appear explicitly in Equation (3).

Using the relation $p=NkT$, where T is the temperature and k is Boltzmann's con-

© Kluwer Academic Publishers • Provided by the NASA Astrophysics Data System

1971SoPh...18..258P

stant, we can eliminate the density from Equations (2) and (3) and, if T is taken to be a constant, integrate the resulting expressions to give

$$pVS = p_0 V_0 S_0 \tag{4}$$

$$\frac{V^2}{2} + \frac{kT}{m} \ln \frac{p}{p_0} + \frac{GM_\odot}{r_0}\left(1 - \frac{r_0}{r}\right) = \frac{V_0^2}{2}. \tag{5}$$

Here, p_0, V_0, S_0, denote the pressure, velocity, and cross-section, respectively, of the flux tube at the reference level r_0. It must be kept in mind that these quantities are *not* constants but, in general, are functions of latitude.

Evaluating Equation (5) at the cusp in both the closed and open regions, we find

$$p_c = p_0 \exp\left[-\frac{GM_\odot m}{r_0 kT}\left(1 - \frac{r_0}{r_n}\right)\right]$$

$$p_s = p_0 \exp\left[-\frac{GM_\odot m}{r_0 kT}\left(1 - \frac{r_0}{r_n}\right) + \frac{m(V_0^2 - V_n^2)}{2kT}\right]$$

where r_n is the radial distance to the neutral point and V_n is the velocity there.* Writing p_c as a function of p_s and substituting into Equation (1) gives

$$p_c - p_s = p_s\left\{\exp\left[\frac{m(V_n^2 - V_0^2)}{2kT}\right] - 1\right\} = \frac{B_s^2}{8\pi}. \tag{6}$$

If the helmet top is some distance above the solar surface but still well below the sonic point (this is the case for observed streamers), then $V_0^2 \ll V_n^2 \ll 2kT/m$ and Equation (6) reduces approximately to

$$V_n^2 \approx \frac{2kTB_s^2}{8\pi m p_s} = \frac{B_s^2}{4\pi m N_s} = V_a^2$$

where N_s is the number density in the streaming region at the neutral point and V_a is the local Alfvén speed there. That is, for the expansion just outside the closed region, *the transformation from sub-Alfvénic to super-Alfvénic velocity occurs at the cusp.*

3. Numerical Techniques

The problem before us is to determine numerically the properties (density, temperature, velocity, magnetic field, etc.) of a model corona subject to appropriate boundary conditions at the coronal base. As mentioned earlier, the necessary boundary conditions are density, temperature, and normal component of the magnetic field. For the purposes of this work we will approximate the corona as being isothermal and symmetric about the rotation axis. Moreover, we neglect the effects of solar rotation since these are not expected to have a significant influence on the poloidal components of the field and velocity.

The differential equations to be solved are highly non-linear and, rather than

* Since we choose the reference level to be low in the corona, the reference pressure is nearly the same on either side of the interface between the two regions.

© Kluwer Academic Publishers • Provided by the NASA Astrophysics Data System

1971SoPh...18..258P

being purely hyperbolic or elliptic, are mixed in character. Consequently, standard methods for solving partial differential equations are of little use here. We employ an iterative technique consisting of three steps. This method makes use of the fact that, for specified electric currents, the equation determining the magnetic field distribution is elliptic. Moreover, for a specified magnetic field distribution, the flow along individual field lines may be calculated by total differential equations, independent of conditions on neighboring field lines. The three steps of the iteration are described below.

Step 1 – Determination of the magnetic field for a known distribution of electric currents. To begin the iteration an initial distribution of electric currents is specified throughout all space. The magnetic field consistent with these currents is calculated as follows. Since $\nabla \cdot \mathbf{B} = 0$, we can write $\mathbf{B}$ as the curl of the vector potential $\mathbf{A}$:

$$\mathbf{B} = \nabla \times \mathbf{A}. \tag{7}$$

The differential equation determining $\mathbf{A}$ from a known current $\mathbf{J}$ is

$$\nabla \times (\nabla \times \mathbf{A}) = 4\pi \mathbf{J}. \tag{8}$$

For the case of axial symmetry, Equation (8) becomes particularly simple since both $\mathbf{A}$ and $\mathbf{J}$ have only azimuthal components A and J, respectively. It is convenient to introduce new independent variables $y = r_0/r$ and $\mu = \cos\theta$, where θ is the colatitude. In the y, μ-plane, all physical space for $r > r_0$ is transformed into a finite rectangular region $0 < y < 1$ and $-1 < \mu < 1$. Using the definitions

$$f = A \sin\theta / r_0 B_{0p}$$
$$j = 4\pi r_0 J / B_{0p},$$

where B_{0p} is the magnetic field strength at $r = r_0$ and at the pole ($\theta = 0$), Equation (3) becomes

$$y^2 \frac{\partial^2 f}{\partial y^2} + (1 - \mu^2) \frac{\partial^2 f}{\partial \mu^2} = - \frac{(1 - \mu^2)^{1/2}}{y^2} j. \tag{9}$$

To simplify the discussion, we will restrict ourselves to magnetic field distributions which are not only axisymmetric, but also symmetric about the equator (the polarity is, of course, of the opposite sign in the two hemispheres). For this case it is known *a priori* that the neutral point and neutral sheet lie on the equator. Also, symmetry allows us to consider only the square $0 \leqslant y \leqslant 1$, $0 \leqslant \mu \leqslant 1$ bounded by the solar surface, the pole, infinity, and the equator. Equation (9) is a linear elliptic differential equation and, consequently, its solution is fixed by specifying either the value of f or its normal derivative everywhere on the boundaries of this square box and j as a function of position in the interior.

At the reference level ($y = 1$), f can be written in terms of the normal component of B there. Also, f must vanish at the pole ($\mu = 1$) and at infinity ($y = 0$). Hence, the

© Kluwer Academic Publishers • Provided by the NASA Astrophysics Data System

1971SoPh...18..258P

boundary values of $f(y, \mu)$ on these three sides are

$$f(1, \mu) = -\int_1^{\mu} b_0(\mu)\, d\mu \tag{10}$$

$$f(y, 1) = f(0, \mu) = 0, \tag{11}$$

where $b_0(\mu) = B_N(\mu)/B_{0_p}$, $B_N(\mu)$ being the normal component of the magnetic field at $y = 1$.

The boundary conditions to be applied on the remaining boundary $\mu = 0$ (solar equator) is more complicated. Suppose the value of y at which the neutral point occurs is denoted as y_N and the value of f there is f_N (both y_N and f_N are yet to be determined). Then, along the neutral sheet ($0 \leqslant y \leqslant y_N$) no field lines can cross the equator. This is equivalent to the condition that $\partial/\partial y[f(y, 0)/y] = 0$ for $y < y_N$. Integrating, we obtain the boundary value for f along the neutral sheet in terms of the two yet undetermined parameters y_N and f_N

$$f(y, 0) = (f_N/y_N)y \quad \text{for} \quad 0 \leqslant y \leqslant y_N. \tag{12}$$

Below the neutral point, the field lines must cross the equator perpendicularly. This requires that

$$\partial f/\partial \mu\,(y, 0) = 0 \quad \text{for} \quad y_N \leqslant y \leqslant 1. \tag{13}$$

We have now specified either f or its derivative everywhere along the boundaries of the box in terms of the still arbitrary constants y_N and f_N. y_N and f_N are determined by two additional constraints. Equation (12) assures that B_θ (component of B perpendicular to the equator) vanishes along the neutral sheet. However, for arbitrary values of y_N and f_N, B_θ will not got to zero when approaching the neutral point from the inside ($y > y_N$). Mathematically, this condition can be written as

$$\lim_{\varepsilon \to 0} \frac{\partial}{\partial y}\left(\frac{f}{y}\right)\Bigg|_{y = y_N + \varepsilon} = 0. \tag{14}$$

Also, in line with the discussion of Section 2, the neutral point must be of the 'cusp-type', requiring that

$$\lim_{\varepsilon \to 0} \frac{\partial^2}{\partial y^2}\left(\frac{f}{y}\right)\Bigg|_{y = y_N + \varepsilon} = 0. \tag{15}$$

A diagram of the y, μ-plane showing all the imposed conditions is shown in Figure 2.

In practice, the solution of Equation (9) is carried out by dividing the box into a mesh of evenly spaced points in y and μ, specifying the value of j at each mesh point, and employing a 4-point relaxation method. During the relaxation, y_N and f_N are continually adjusted so as to satisfy conditions (14) and (15). Hence, the boundary condition along the equator is in a sense a floating boundary condition which varies during the relaxation and depends upon the solution itself.

© Kluwer Academic Publishers • Provided by the NASA Astrophysics Data System

1971SoPh...18..258P

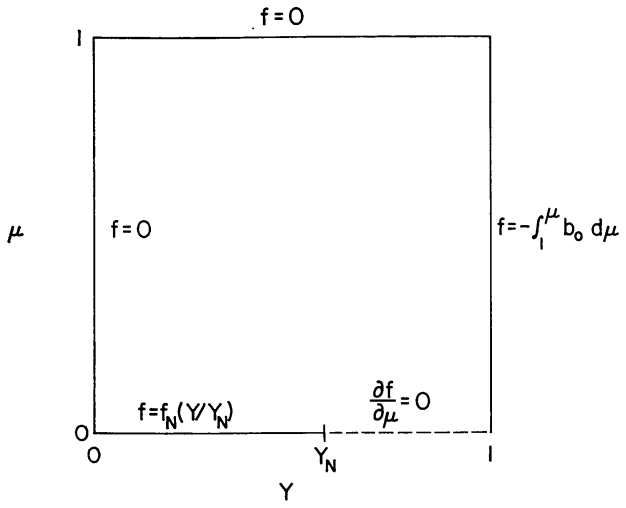


Fig. 2. A pictorial representation of the y, μ coordinate space showing the appropriate boundary conditions on f to be applied on all the boundaries.

For a given set of electric currents, only one out configuration exists satisfying Equations (10) through (15).* Once this solution for f is obtained, the magnetic field distribution can be easily found from Equation (7).

Step 2 – Solution of the solar wind equations. The magnetic field distribution found in step 1 is now used to define a streamtube geometry in which the relevent solar wind equations can be solved along each individual field line. To do this, it is convenient to use our natural coordinate system in which s is the coordinate along the field and n the coordinate normal to the field.** Since $\nabla \cdot \mathbf{B} = 0$, the variation of cross-sectional area, S, along any flux tube is then given in terms of the magnetic field by

$$S(s) = S_0 B_0 / B(s)$$

where B_0 is the magnetic field strength at the reference level.

The equations to be solved in this step are Equations (4) and (5). Along a closed field line, we take $V = V_0 = 0$ and Equation (5) yields

$$p = p_0 \exp\left[-\frac{GM_\odot m}{r_0 kT} (1 - y) \right]$$

This simply states that hydrostatic equilibrium holds along the field.† On open field lines, the additional constant V_0 appears. V_0 is adjusted for each field line to obtain the so-called 'critical solution', that is, the solution for which the flow begins near the

* As the electric currents approach zero everywhere, $y_N \to 0$ indicating that the neutral point moves out to infinity. One thus obtains, in the limit of zero current, the expected potential field with no open field lines.

** Although the present analysis is for isothermal conditions, the energy equation is also simplest in this coordinate system since conduction takes place, to a high degree of approximation, only along field lines.

† By this we mean that p and p_0 must be measured along the same field line.

© Kluwer Academic Publishers • Provided by the NASA Astrophysics Data System

1971SoPh...18..258P

Sun with a subsonic velocity, passes smoothly through the sonic point, and is supersonic at large distances.

For a given field line geometry found in step 1, Equations (4) and (5) yield unique solutions for N and V in both closed and open magnetic regions as a function of the temperature T and the latitude distribution of density $N_0(\mu)$ at the reference level.

Step 3 – Derivation of new electric currents. The integration of Equations (4) and (5) insures the conservation of mass and momentum along the field lines. However, the equilibrium of forces *normal* to the field has not yet been imposed. We now utilize this condition to derive new electric currents.

For the case of axial symmetry $\mathbf{J}\cdot\mathbf{B}=0$. Taking the vector cross product of the momentum equation with $\mathbf{B}$ one obtains

$$\left[mN(\mathbf{V}\cdot\nabla)\mathbf{V}+\nabla p+\frac{GM_\odot m}{r^2}N\hat{\mathbf{e}}_r\right]\times\mathbf{B}=(\mathbf{J}\times\mathbf{B})\times\mathbf{B}=-B^2\mathbf{J} \tag{16}$$

where $\hat{\mathbf{e}}_r$ is a unit vector in the radial direction. Hence, the azimuthal current $\mathbf{J}$ necessary to produce a $\mathbf{J}\times\mathbf{B}$ force which balances the components of the inertial, pressure, and gravitational forces normal to the field can be found from Equation (16). With some manipulation, this equation can be written in the more physically illuminating form

$$J=-\frac{1}{B}\left[\frac{\partial p}{\partial n}+\frac{GM_\odot m}{r^2}N\sin\alpha+\frac{mNV^2}{R}\right]. \tag{17}$$

Here, $\partial p/\partial n$ represents the pressure gradient normal to the field, the second term on the right-hand side is the component of the gravitational force normal to the field, and the last term is the centrifugal force (R being the radius of curvature of the field line).

The sheet current J^* between the open and closed field lines can be derived either from Equation (16) or from the equivalent condition that $p+B^2/8\pi$ be continuous across the interface. Since $J^*=[B]/4\pi$ (the brackets denoting the jump in a quantity across an interface), we have

$$\begin{aligned}\left[p+\frac{B^2}{8\pi}\right]&=[p]+\frac{1}{8\pi}[B^2]\\&=[p]+\frac{1}{8\pi}(B_c+B_s)[B]\\&=[p]+\tfrac{1}{2}(B_c+B_s)J^*=0,\end{aligned}$$

where B_c and B_s represent the field at the boundaries of the closed and streaming regions respectively. This yields an expression for J^* in terms of the known magnetic field and the pressure discontinuity produced by the flow*.

The calculation of new currents everywhere completes one iteration, whereupon we

* For purposes of computation in step 1, this sheet current is converted into equivalent weighted volume currents at the two mesh points immediately adjacent to the interface. Hence, this current becomes a true sheet current only in the limit of an infinitely fine mesh.

© Kluwer Academic Publishers • Provided by the NASA Astrophysics Data System

1971SoPh...18..258P

return to step 1 and continue the process. The iteration is considered converged when the field found in step 1 differs from that found on the previous iteration by some prescribed small amount.

4. A Numerical Example

In this section, we present the results of applying the iterative technique described above to a situation which is simple, yet which still adequately demonstrates the essential physics. We take the normal component of the magnetic field at the coronal base to be that of a dipole ($B_N = B_{0p} \cos\theta$) and the density there to be independent of latitude. The coronal temperature is taken as 1.56×10^6 K and the magnitude of the reference density is chosen such that the gas pressure at the reference level is equal to the magnetic pressure at that level at the pole ($p_0 = B_{0p}^2/8\pi$). The mean molecular weight is chosen to be 0.608 corresponding to a 10:1 hydrogen-helium ratio. The magnitude of B_{0p} is taken as 1 G.

The resultant converged solution is depicted in Figure 3. The appearance of the configuration is similar in many respects to the large helmet streamers observed at solar eclipses with the region of closed loops extending out to about 2.5 $R_\odot$ and the field everywhere being pulled outward by the solar wind.*

A more instructive illustration than Figure 3 is Figure 4 which shows the same solution in the y, μ coordinate system. In this system, the solution over all space outside the Sun can be presented in a finite area. The top and bottom boundaries here ($\mu = \pm 1$) represent the north and south poles respectively, the right-hand boundary ($y = 1$) the solar surface, and the left-hand boundary ($y = 0$) infinity. It is evident here

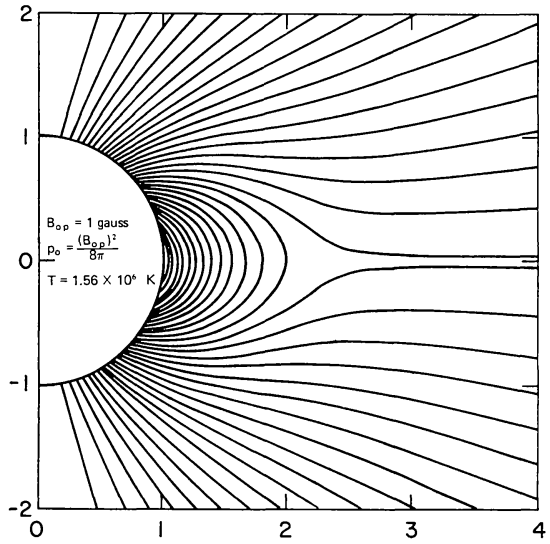


Fig. 3. Field and streamline distribution corresponding to base conditions in which the normal component of the magnetic field is that of a dipole and the reference density is independent of latitude.

* Due to the scale height effect, the height at which the field lines open is most sensitive to the coronal temperature.

© Kluwer Academic Publishers • Provided by the NASA Astrophysics Data System

1971SoPh...18..258P

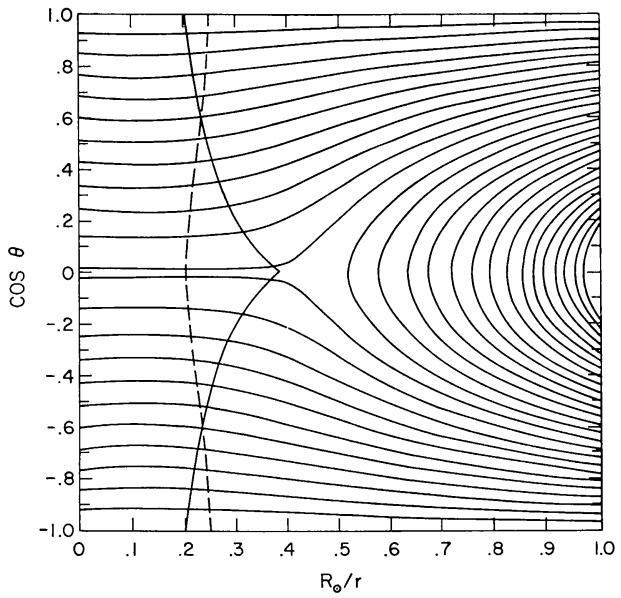


Fig. 4. The same field configuration as in Figure 3 but plotted in y, μ space. The nearly vertical dashed curve depicts the sonic surface while the solid curve represents the Alfvénic surface.

that the field becomes asymptotically radial at large distances. The vertical dashed curve represents the sonic surface (where the velocity passes through the speed of sound) and the solid curve the Alfvénic surface (where the flow passes through the Alfvén speed). The sonic surface is at 4 $R_\odot$ at the pole and moves out to 5 $R_\odot$ near the equator. The Alfvénic surface, on the other hand, is at about 5 $R_\odot$ at the pole and moves in to the neutral point ($\approx 2.5\ R_\odot$) at the equator as expected from the discussion of Section 2.

In Figure 5, the nondimensional velocity, u, is shown as a function of radial distance along two separate field lines. The solid curve represents the flow out along the pole whereas the dashed curve is the velocity along a field line near the closed region. Note that the velocity increases from pole to equator below the cusp but decreases toward the equator at larger distances. This qualitative difference in velocity variation is explained by the fact that the flux tube cross-section below the neutral point expands slower near the pole than near the closed region. Above the neutral point the opposite is true.

Figure 6 shows the latitude distribution of volume current at a typical level below the neutral point. The current is, of course, zero at the pole, increases to a maximum positive value, then becomes negative near the closed region. The large positive spike is due to the sheet current (converted to equivalent volume currents as discussed in Section 3) at the interface between the closed and open field lines. The current density is zero inside the helmet *only* in this special case where the base pressure is independent of latitude.*

The current distribution above the helmet top is depicted in Figure 7. Here, the

* In this case, hydrostatic equilibrium can be satisfied normal to the field as well as along the field, and no *local* interaction takes place between the gas and magnetic field.

© Kluwer Academic Publishers • Provided by the NASA Astrophysics Data System

1971SoPh...18..258P

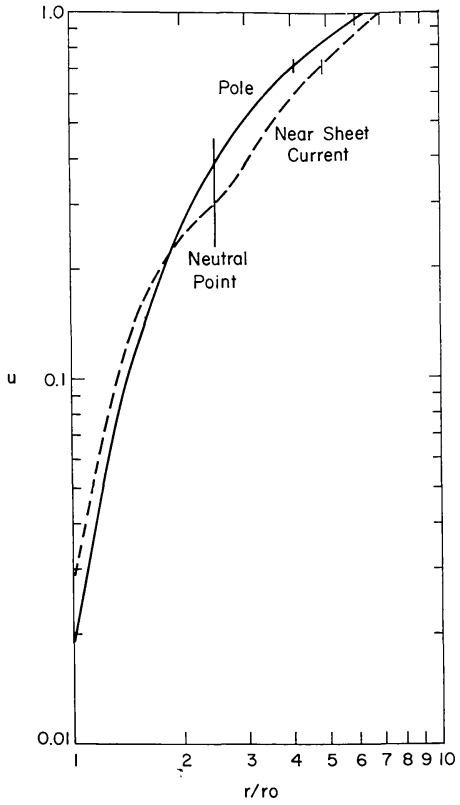


Fig. 5. Radial dependence of the nondimensional velocity u [$= V/(2kT/m)^{1/2}$] along open field lines emanating from the pole (solid curve) and from near the sheet current separating the open and closed regions (dashed curve). The point at which $u = 1/\sqrt{2}$ is the critical point and is indicated by a short vertical bar on each curve. The location of the neutral point is shown by the long vertical bar.

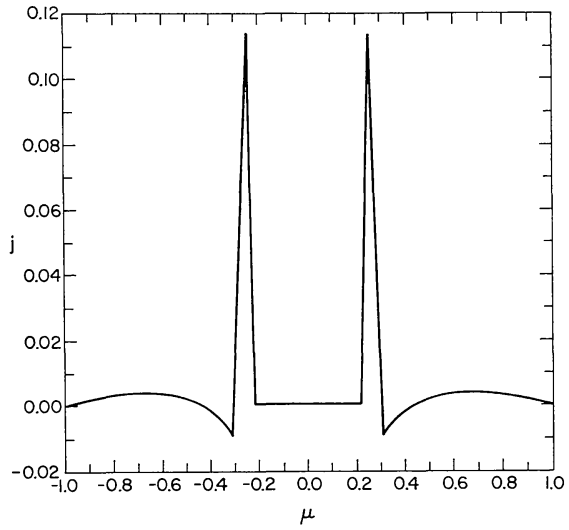


Fig. 6. Variation of nondimensional current density j with latitude at a typical level below the neutral point. The large positive spike is the sheet current at the interface separating the open and closed field lines.

© Kluwer Academic Publishers • Provided by the NASA Astrophysics Data System

1971SoPh...18..258P

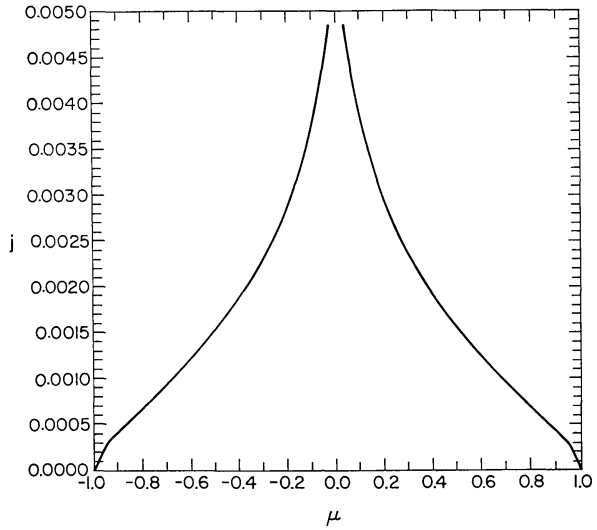


Fig. 7. Typical latitude variation of current density above the cusp.

current increases monotonically from zero at the pole to its maximum value at the equator.

Figure 8 shows a comparison of the field lines of our computed model with those of a potential field with the same normal component at the reference level. To make the comparison meaningful, the field lines for the two cases are chosen so as to be coincident at the surface. As expected, the field is everywhere stretched outward by the gas with this distention becoming large near the neutral point.

In the closed region well below the cusp the difference between the two configurations is small, *mainly because the pressure at the reference level is taken to be independent of latitude*. The outward distention of the field in this region, as a result, is produced solely by currents generated by the expansion along open field lines. For

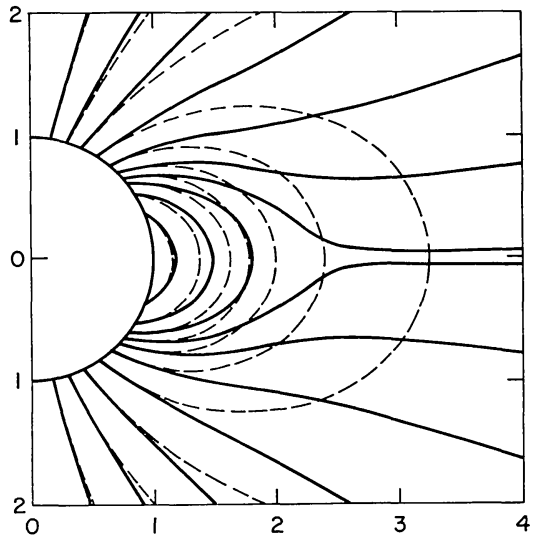


Fig. 8. A comparison of the magnetic field of Figure 3 (solid curves) with a potential field (dashed curves) having the same normal component at the reference level. The field lines for the two configurations are chosen so as to be coincident at the surface.

© Kluwer Academic Publishers • Provided by the NASA Astrophysics Data System

1971SoPh...18..258P

the general case of variable surface pressure, however, a pressure and gravitational force balance cannot be satisfied normal to the field and significant $\mathbf{J} \times \mathbf{B}$ forces (if $p \approx B^2/8\pi$) are expected to maintain the equilibrium.

5. Conclusions

The results of Section 4 apply only to an extremely simple physical situation, symmetric both to the rotational axis and the equator. Nevertheless, they demonstrate the possibility of numerically modeling the structure and physical properties of the solar corona and interplanetary medium as functions of measured quantities at the coronal base. The obvious extensions which must be made are the inclusion of the energy equation within the framework of the model as well as relaxing the symmetry conditions imposed here. When this is done, more realistic surface distributions of magnetic field and density can be treated.

It should finally be pointed out, however, that the iterative technique described here requires considerable storage capacity and computing time on large electronic computers. It may well be that this consideration will be the limiting factor when modeling actual solar conditions.

Acknowledgements

The authors wish to extend special thanks to Nancy Werner who wrote the computer program upon which this work is based. Thanks are also extended to Friedrich Meyer and Gordon Newkirk, Jr. for constructive discussions during the course of this work and to F. Q. Orrall and M. Raadu for reviewing the manuscript.

References

Kuperus, M.: 1965, *Res. Astron. Observ. Utrecht* **17**, 1.
Meyer, F. and Schmidt, H. U.: 1968, *Angew. Math. Mech.* **48**, 218.
Newkirk, G. and Altschuler, M. D.: 1970, *Solar Phys.* **13**, 131.
Osterbrock, D. E.: 1961, *Astrophys. J.* **134**, 347.
Pneuman, G. W. and Kopp, R. A.: 1970, *Solar Phys.* **13**, 176.
Sturrock, P. A. and Smith, S. M.: 1968, *Solar Phys.* **5**, 87.

© Kluwer Academic Publishers • Provided by the NASA Astrophysics Data System